Oral Oncology 46 (2010) 748–754

Contents lists available at ScienceDirect

Oral Oncology

journal homepage: www.elsevier.com/locate/oraloncology

A novel indole-3-carbinol derivative inhibits the growth of human oral squamous cell carcinoma *in vitro*

Jing-Ru Weng [a,*], Li-Yuan Bai [b,c], Hany A. Omar [d], Aaron M. Sargeant [e], Ching-Tung Yeh [a], Yuan-Yin Chen [a], Ming-Hsui Tsai [b], Chang-Fang Chiu [c,f]

[a] *Department of Biological Science and Technology, China Medical University, Taichung 40402, Taiwan*
[b] *Graduate Institute of Clinical Medical Science, China Medical University, Taichung 40402, Taiwan*
[c] *Division of Hematology and Oncology, Department of Internal Medicine, China Medical University Hospital, Taichung 40402, Taiwan*
[d] *Department of Pharmacology, Faculty of Pharmacy, Beni-Suef University, 62511, Egypt*
[e] *Charles River Laboratories, Preclinical Services, Spencerville, OH 45887, USA*
[f] *Cancer Center, China Medical University Hospital, Taichung 40402, Taiwan*

ARTICLE INFO

Article history:
Received 28 June 2010
Received in revised form 9 August 2010
Accepted 9 August 2010
Available online 16 September 2010

Keywords:
Indole-3-carbinol
OSU-A9
Oral cancer
Akt
NF-κB
Apoptosis

SUMMARY

Indole-3-carbinol (I3C), a naturally occurring phytochemical found in cruciferous vegetables, has received much attention due to its translational potential in cancer prevention and therapy. In this study, we investigated the antitumor effects of OSU-A9, a structurally optimized I3C derivative, in a panel of oral squamous cell carcinoma cell lines, SCC4, SCC15, and SCC2095. The antiproliferative effect of OSU-A9 was approximately two-orders-of-magnitude higher than that of I3C. Importantly, normal human oral keratinocytes were less sensitive to OSU-A9 than oral cancer cells. This antiproliferative effect of OSU-A9 was attributable to the induction of mitochondrial-dependent apoptosis as evidenced by sub-G1 accumulation of cells, poly ADP-ribose polymerase cleavage, and cytochrome *c* release from the mitochondria. OSU-A9 down regulates Akt and NF-κB signaling pathways, leading to changes in many downstream effectors involved in regulating cell cycle and apoptosis. Moreover, the observed down regulation of IKKα and IKKβ expression by OSU-A9 is not reported for I3C. OSU-A9 also induces both the production of reactive oxygen species and the endoplasmic reticulum stress. Taken together, these results suggest the translational value of OSU-A9 in oral squamous cell cancer therapy in the future.

Introduction

Although the mechanisms underlying the development of oral squamous cell carcinoma are not fully understood, tobacco use, alcohol, and betel quid chewing are the major risk factors in Taiwan. Radical surgery, followed by chemoradiation, represents the main treatment approach for this disease. The prognosis is dismal for patients with metastatic disease even with the use of chemotherapeutic agents including platinum, 5-fluorouracil, taxane, ifosfamide, and methotrexate.[1] These patients succumb eventually to their disease once resistance to these chemotherapeutic agents is developed. This highlights the necessity to develop novel compounds or strategies for patients with advanced oral squamous cell carcinoma.

Indole-3-carbinol (I3C), a natural phytochemical found in the vegetables of the cruciferous family, has been shown to suppress the proliferation of cancer cells of breast, colon, prostate, and endometrium by targeting multiple signaling pathways.[2–5] In addition, I3C shows a synergistic effect when combined with 1,3-tetradecanoyl phorbolacetate plus $CaCl_2$ against oral squamous cell carcinoma cell lines.[6] However, there are several drawbacks for I3C as an anticancer agent. First, the effective concentration of I3C to exert its antitumor activity is between 50 and 100 μM, which is impractical *in vivo*. Second, the chemical instability of I3C and vulnerability to acid-catalyzed conversion into a variety of derivatives in the stomach decrease its antitumor activity.[7] Third, the inability to reliably monitor I3C concentration in plasma limits its pharmacokinetic anaylsis.[8] Consequently, the structural modification of I3C or 3,3′-diindolylmethane attracted many researchers to develop novel indole derivatives with improved potency.[5,9] Among these derivatives, OSU-A9, an acid-stable analogue with higher apoptosis-inducing potency was synthesized.[10] OSU-A9 has been reported to be active against cancers of prostate, breast and liver *in vitro*, and has inhibited tumor growth of these cancers in xenograft animal models. Importantly, the repeated daily administration of OSU-A9 to athymic nude mice in these experiments was well tolerated.[10–12] In the present study, we compared the

* Corresponding author. Address: Department of Biological Science and Technology, China Medical University, 91 Hsueh-Shih Road, Taichung 40402, Taiwan. Tel.: +886 4 22053366x2511; fax: +886 4 22071507.
E-mail address: columnster@gmail.com (J.-R. Weng).

1368-8375/$ - see front matter © 2010 Elsevier Ltd. All rights reserved.
doi:10.1016/j.oraloncology.2010.08.005

in vitro efficacy of OSU-A9 with that of I3C against three oral squamous cell carcinoma cell lines. The possible mechanisms underlying the anticancer activity of OSU-A9 against oral squamous cell carcinoma cells are also investigated.

Materials and methods

Cell culture

SCC4, SCC9, and SCC2095 human oral cancer cells were kindly provided by Professor Susan R. Mallery (The Ohio State University), and were cultured in DMEM/F12 medium (Gibco, Grand Island, NY) supplemented with 10% fetal bovine serum and penicillin (100 U/mL)/streptomycin (100 μg/mL) (Invitrogen, Carlsbad, CA). Normal human oral keratinocytes (NHOK) were kindly provided by Dr. Tzong-Ming Shieh (China Medical University) and were maintained in the keratinocyte serum-free medium (Gibco, Grand Island, NY). All cell types were cultured at 37 °C in a humidified incubator containing 5% CO_2.

Reagents

OSU-A9 {[1-(4-chloro-3-nitrobenzene-sulfonyl)-1*H*-indol-3-yl]-methanol} was synthesized as previously described,[10] with identity and purity ($\geqslant$99%) verified by proton nuclear magnetic resonance, high-resolution mass spectrometry, and elemental analysis. I3C was purchased from Sigma–Aldrich. For *in vitro* experiments, both agents were dissolved in dimethyl sulfoxide (DMSO), and added to the culture medium with a final DMSO concentration less than 0.1%.

Cell viability analysis

The cell viability was assessed using the MTT [3-(4,5-dimethylthiazol-2-yl)-2,5-diphenyl-2*H*-tetrazolium bromide] assay in six replicates. The cells (5×10^3/200 μL) were seeded in 96-well, flat-bottomed plates for 24 h, and were then exposed to various concentrations of test agents for the indicated time intervals. After removing the culture medium, 200 μL of the medium containing MTT at a concentration of 0.5 mg/mL was added, and the cells were incubated at 37 °C for 2 h. The medium was removed and the reduced MTT dye in each well was dissolved in 200 μL DMSO. Absorbance was determined with a multi-mode microplate reader Synergy HT (Bio-Tek) at 570 nm.

Cell cycle and apoptosis analysis

SCC2095 cells (2×10^5/3 mL) were treated with the indicated concentration of OSU-A9 or I3C for 48 h. After being washed twice with ice-cold phosphate-buffered saline (PBS), the cells were fixed in 70% cold ethanol for 4 h at 4 °C. For cell cycle analysis, the cells were stained with propidium iodide and analyzed by the multicycler software. For apoptosis evaluation, the cells were stained with 4,6-diamidino-2-phenylindole (DAPI) and analyzed using BD FACSAria flow cytometer (Becton Dickinson, Germany).

Mitochondrial membrane potential ($\Delta\Psi m$) and reactive oxygen species (ROS) generation

Briefly, the cells (2×10^5/3 mL) were treated with DMSO or different concentrations of OSU-A9 for 48 h and washed with PBS twice. The cells were stained by DiOC6 (40 nM) and by DCFH-DA (5 μM) for 30 min for mitochondrial membrane potential ($\Delta\Psi$m) and ROS determination, respectively. Cells in both the analyses were assessed by fluorescence intensity using flow cytometer (Becton Dickinson, Germany).

Western blotting

Cell lysates were prepared by adding cells with RIPA buffer (50 mM Tris pH 8.0, 150 mM NaCl, 1% NP40, 0.5% sodium deoxycholate, and 0.1% sodium dodecyl sulfate). Protease inhibitor (Sigma, Saint Louis, MO) and phosphatase inhibitor cocktail (Calbiochem, Gibbstown, NJ) were added to RIPA buffer before lysing the cells. Protein concentrations of cell lysates were measured using Bio-Rad protein assay dye reagent (BIO-RAD Laboratories, Hercules, CA). The mixture solution of Laemmli sample buffer (BIO-RAD, 62.5 mmol/L Tris–HCl, pH 6.8, 2% sodium dodecyl sulfate, 25% glycerol, and 0.01% bromphenol blue) and β-mercaptoethanol (19:1) was added to the lysates, and the lysates were boiled at 95 °C for 10 min. Equal amounts of protein lysates were separated using sodium dodecyl sulfate–polyacrylamide gel electrophoresis and transferred to nitrocellulose membranes (Hyperbond ECL, GE Healthcare, Piscataway, NJ). After blocking with TBST (TBS containing 0.1% Tween 20) containing 5% nonfat milk for 1 h, the membranes were incubated with the indicated primary antibodies at 4 °C overnight. The membrane was washed five times with TBST and then incubated with horseradish peroxidase (HRP)-conjugated goat anti-mouse IgG antibodies or goat anti-rabbit IgG antibodies (Jackson ImmunoResearch) for 1 h at room temperature. After five washes with TBST, the blots were visualized with the enhanced chemiluminescence Amersham ECL Western Blotting Detection Reagents (GE Healthcare, Piscataway, NJ). Primary antibodies against various biomarkers were obtained from the following sources: p-^{473}Ser Akt, p-^{308}Ser Akt, cyclin D1, XIAP, COX IV, IKKα, IKKβ, IκBα, p-^{32}Ser IκBα, Bad, p-^{112}Ser Bad, and NF-κB (Cell Signaling Technologies, Beverly, MA); Akt, p27, p21, Bax, Bcl-2, and Bcl-xL (Santa Cruz Biotechnology, Santa Cruz, CA); survivin (R&D Systems, Minneapolis, MN); β-actin (Sigma–Aldrich, St. Louis, MO).

NF-B-dependent reporter gene expression assay

The expression activity was determined as previously described.[11,12] Briefly, SCC2095 cells were co-transfected with 2 μg of the p-NF-κB-Luc reporter plasmid and 0.5 μg of the Renilla Luciferase Control Reporter Vector (p-RL-CMV, Promega) using

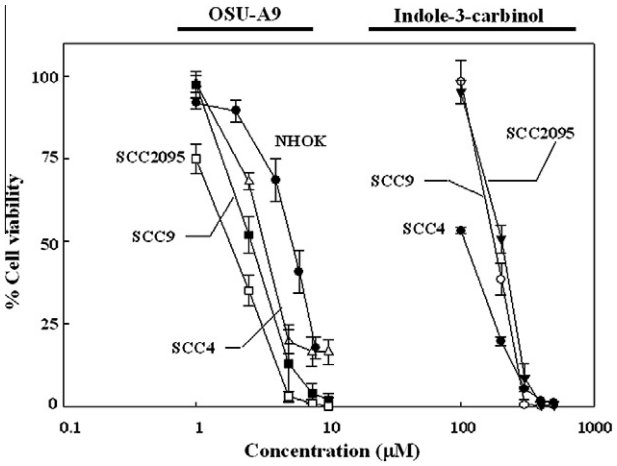

Figure 1 Antiproliferative effects of OSU-A9 and indole-3-carbinol in three oral cancer cell lines (SCC4, SCC9, SCC2095) and normal human oral keratinocytes (NHOK). Cells (5×10^3/200 μL) were treated with OSU-A9 or indole-3-carbinol for 48 h, and cell viability was assessed by MTT assays ($n = 6$).

the Amaxa® Nucleofector system (Gaithersburg, MD). The transfected cells were incubated in 12-well plates for 24 h. The cells were treated in triplicate with the indicated concentrations of OSU-A9 or DMSO in the presence of vehicle or 0.1 μM TNF-α (Pepro Tech,

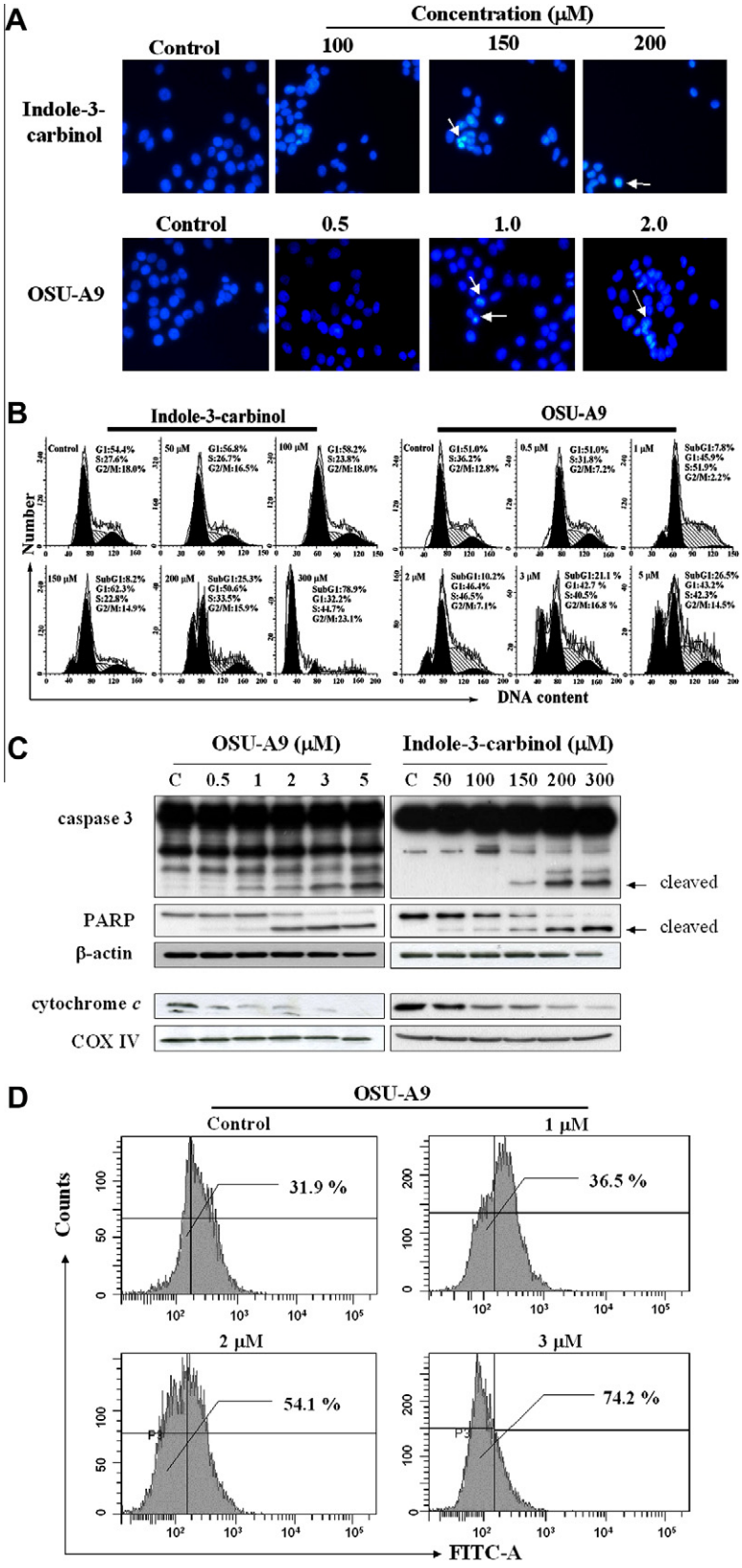

Figure 2 OSU-A9 and indole-3-carbinol (I3C) induced apoptosis through the mitochondrial pathway in SCC2095 cells. DAPI staining showed apoptotic cells with pyknotic nuclei featuring intense bluish-white fluorescence (A). Cell cycle analysis showed increased sub-G1 phase in cells treated with OSU-A9 and I3C (B). Western blotting of cell lysates (C, upper panel) and mitochondrial extract (C, lower panel). Mitochondrial membrane potential ($\Delta\Psi m$) was accessed with the fluorescent probe DiOC6 (D). (For interpretation of the reference to color in this figure legend, the reader is referred to the web version of this article.)

Rocky Hill, NJ) for 6 h. The luciferase activities in cell lysates were determined using the Dual-Luciferase Reporter Assay System (Promega, Madison, WI) and normalized to the constitutive renilla luciferase activity.

Fluorescence staining for confocal imaging

Cells (2×10^5/3 mL) were plated on cover slips in each well of a six-well plate. The cells were treated with 0.5 μM OSU-A9 for 48 h with or without 10 nM tumor necrosis factor-α (TNF-α) for 30 min. The cells were fixed in 2% paraformaldehyde for 30 min at room temperature and permeabilized with 0.1% Triton X-100 for 20 min. After blocking with 1% bovine serum albumin (BSA), the cells were incubated with rabbit anti-human NF-κB antibody overnight at 4 °C, followed by incubation with anti-rabbit IgG for 1 h at room temperature. Cells were washed with TBST and then covered before undergoing fluorescent microscopic examination.

Statistical analysis

For comparisons, the effect of OSU-A9 on the luciferase activity of NF-κB in SCC2095 cells was analyzed using one-way analysis of variance followed by the Neuman-Keuls test for multiple comparisons. Differences were considered significant at $P < 0.05$. Statistical analysis was performed using SPSS for Windows (SPSS, Inc., Chicago, IL).

Results

OSU-A9 has a more potent antiproliferative effect than I3C on oral cancer cells

Three oral cancer cell lines, SCC4, SCC9, and SCC2095, were used to investigate the antiproliferative effect of OSU-A9 and I3C. Both I3C and OSU-A9 resulted in a dose-dependent inhibition of cell proliferation in all cell types (Fig. 1). The concentrations of OSU-A9 to inhibit cell growth by 50% were 2.6, 2.4, and 1.4 μM in SCC4, SCC9, and SCC2095, respectively, as compared with 253, 234, and 192 μM for I3C in SCC4, SCC9, and SCC2095, respectively. The concentration of OSU-A9 to result in 50% suppression of cell proliferation in normal human oral keratinocytes (NHOK) was 5.5 μM. Because of the greater activity of OSU-A9 in SCC2095, this cell line was used to perform the following experiments.

OSU-A9 induces apoptosis through the mitochondrial pathway in oral cancer cells

To investigate whether the growth-inhibitory effect of OSU-A9 is due to the induction of apoptosis, DAPI dye staining was conducted in SCC2095 cells treated with either OSU-A9 or I3C for 48 h. The DAPI assay revealed chromatin condensation, which was visualized as intense bluish-white fluorescence in pyknotic nuclei (Fig. 2A). For further confirmation of apoptosis, SCC2095 cells were analyzed by flow cytometry (Fig. 2B). OSU-A9 more potently induced cell accumulation in sub-G1 phase than I3C. For example, OSU-A9 at 3 μM concentration induced 21.1% cells in sub-G1 phase, as compared to 25.3% for I3C at 200 μM. The western blot analysis of SCC2095 cells also revealed a dose-dependent increase in the cleavage of PARP and caspase-3 activation as hallmarks of apoptosis (Fig. 2C).

We next examined whether OSU-A9-induced apoptosis was mediated by the mitochondrial pathway. The protein extracts of mitochondrial fraction were immunoblotted with antibodies against cytochrome *c* and COX IV (Fig. 2C). OSU-A9 exhibited around a 100-fold greater potency in the induction of cytochrome *c* release from mitochondria compared to I3C. Furthermore, SCC2095 cells treated with DMSO or OSU-A9 for 48 h were stained with the fluorescent probe DiOC6 and analyzed for mitochondrial membrane potential ($\Delta\Psi m$). OSU-A9 was able to dissipate the mitochondrial membrane potential in a dose-dependent manner (Fig. 2D).

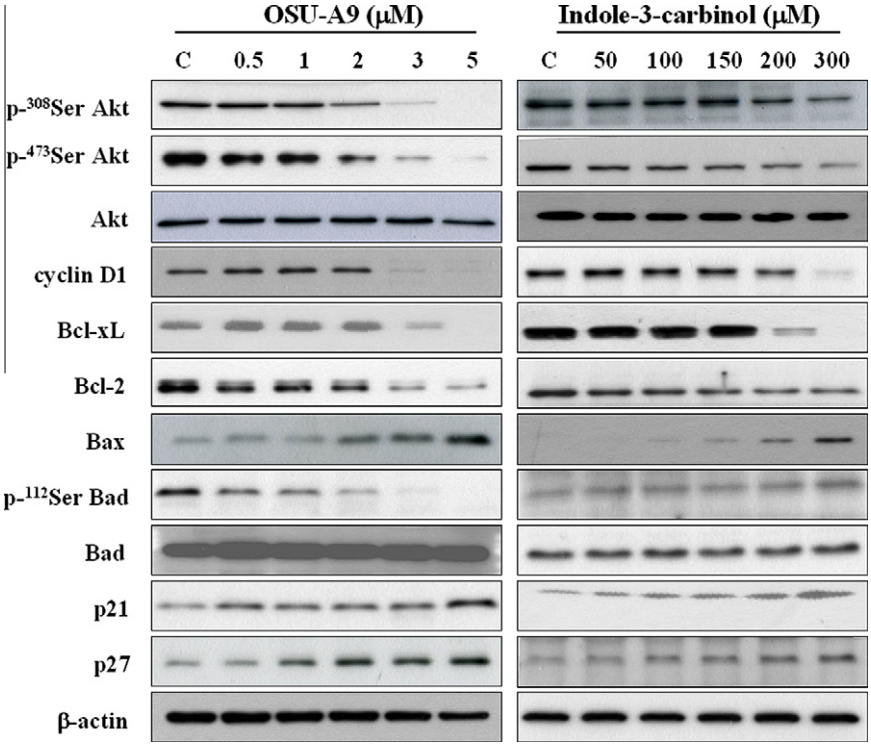

Figure 3 The effect of OSU-A9 on proteins involved in Akt signaling, anti-apoptosis, pro-apoptosis, and cell cycle in SCC2095 cells.

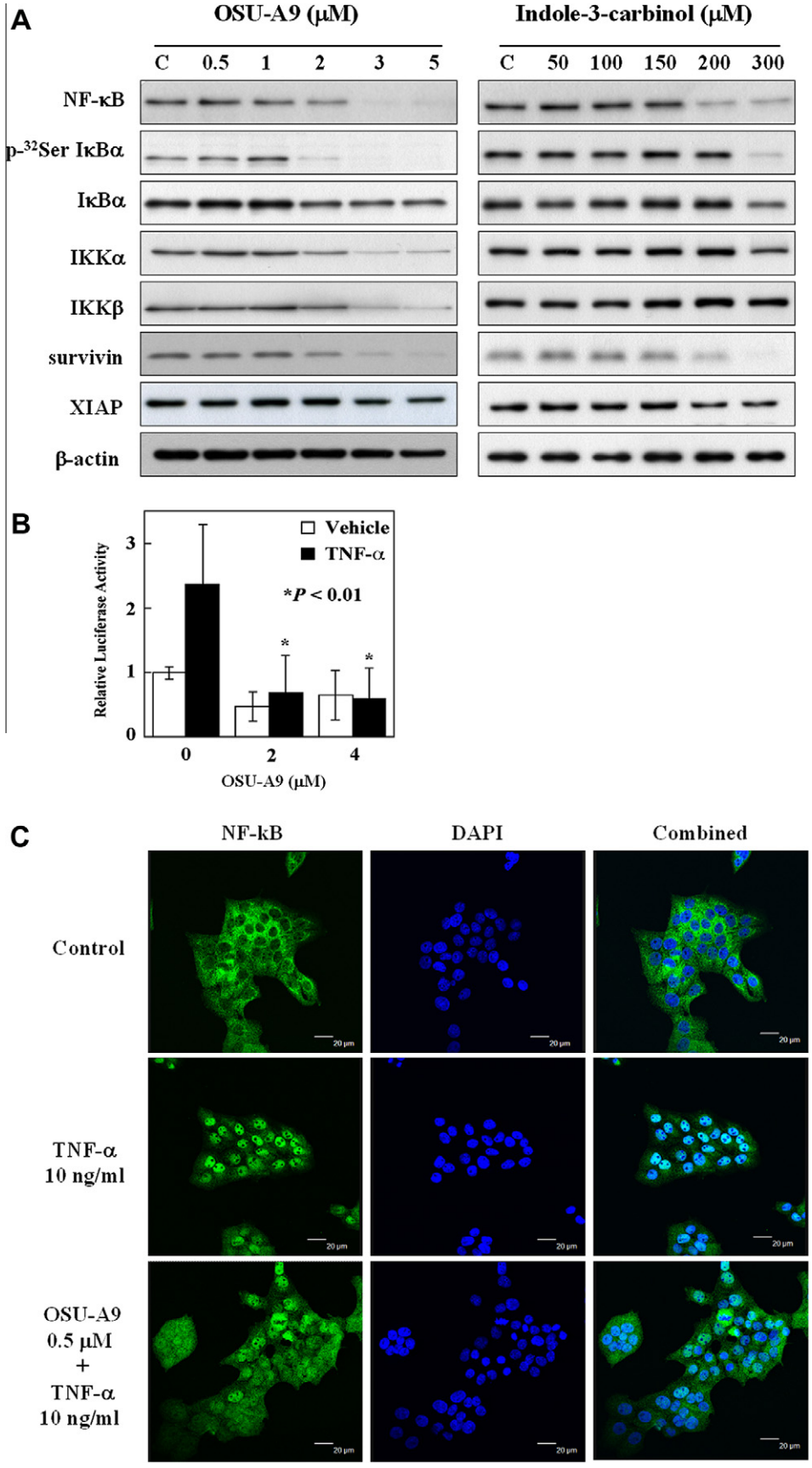

Figure 4 The effect of OSU-A9 on the NF-κB pathway in SCC2095 cells. Western blotting of proteins in the NF-κB pathway (A). NF-κB-luciferase reporter assay. The relative luciferase activities of NF-κB in cells treated with 2 μM and 4 μM of OSU-A9 were compared with those in cells treated with 0 μM of OSU-A9 (B). Confocal microscopic examination (C).

OSU-A9 reduces Akt phosphorylation and cyclin D1 expression

Previous studies showed that Akt and NF-κB signaling pathways were crucial in the anticancer action of I3C.[13,14] In the present study, we found that OSU-A9 induced down regulation of Akt phosphorylation (p-^{473}Ser Akt and p-^{308}Ser Akt) and a downstream effector, cyclin D1, in a dose-dependent manner in SCC2095 cells (Fig. 3). Also, OSU-A9 decreased the expression of antiapoptotic proteins Bcl-xL, Bcl-2, and Bad and increased that of the proapoptotic protein Bax. p21 and p27, two key proteins in regulating cell cycle, were up-regulated in a dose-dependent manner.

OSU-A9 down regulates the NF-B signaling pathway

OSU-A9, as well as I3C, induced down regulation of NF-κB expression (Fig. 4A). Survivin and X chromosome-linked IAP (XIAP), two downstream effectors regulated by NF-κB, were also down modulated by OSU-A9, as was phosphorylated IκBα, which releases NF-κB upon stimulation by upstream p-IKK(α/β). Interestingly, although OSU-A9 treatment resulted in decreased p-IKKα and p-IKKβ, there was no change in the expression of these two proteins after I3C treatment. Furthermore, an NF-κB-luciferase reporter gene assay was used to evaluate the effect of OSU-A9 on tumor necrosis factor-α (TNF-α)-augmented NF-κB signaling. OSU-A9 significantly inhibited NF-κB activation by TNF-α (Fig. 4B). Confocal microscopic examination showed that OSU-A9 at a concentration of 0.5 μM prohibited TNF-α-induced nuclear translocation of NF-κB (Fig. 4C).

OSU-A9 increases ROS and induces endoplasmic reticulum (ER) stress in SCC2095 cells

Previously it had been shown that increased ROS and ER stress were responsible for the activity of some anticancer drugs.[15,16] The evidence that ROS could be induced by ER stress also suggested a crosstalk between ER stress and ROS.[17] Thus we examined the level of ROS in SCC2095 cells treated with OSU-A9 using flow cytometry. OSU-A9 at a concentration of 3 μM significantly increased ROS to 86% from 45% (Fig. 5A, $P < 0.05$). Co-treatment with an antioxidant *N*-acetylcysteine completely rescued the production of ROS induced by OSU-A9. Furthermore, OSU-A9 increased ER stress in SCC2095 cells as evidenced by up regulation of GADD153 and GRP78 expressions in a dose-dependent manner (Fig. 5B).

Discussion

I3C, a natural product found in cruciferous plants, is reported to have antitumor and chemoprevention effects. The main obstacle in its application is the high concentration of I3C required to exhibit physiological functions. We hereby demonstrate that OSU-A9, a novel compound derived from I3C, is more than 100-fold more potent than I3C in inhibiting the growth of oral cancer cells. The action of OSU-A9 is mediated through down regulation of the Akt pathway, modulation of constitutive and inducible NF-κB activation, and induction of ROS and ER stress. Most importantly, the *in vivo* therapeutic application of OSU-A9 is also supported by the fact that normal human oral keratinocytes are less sensitive to the compound.

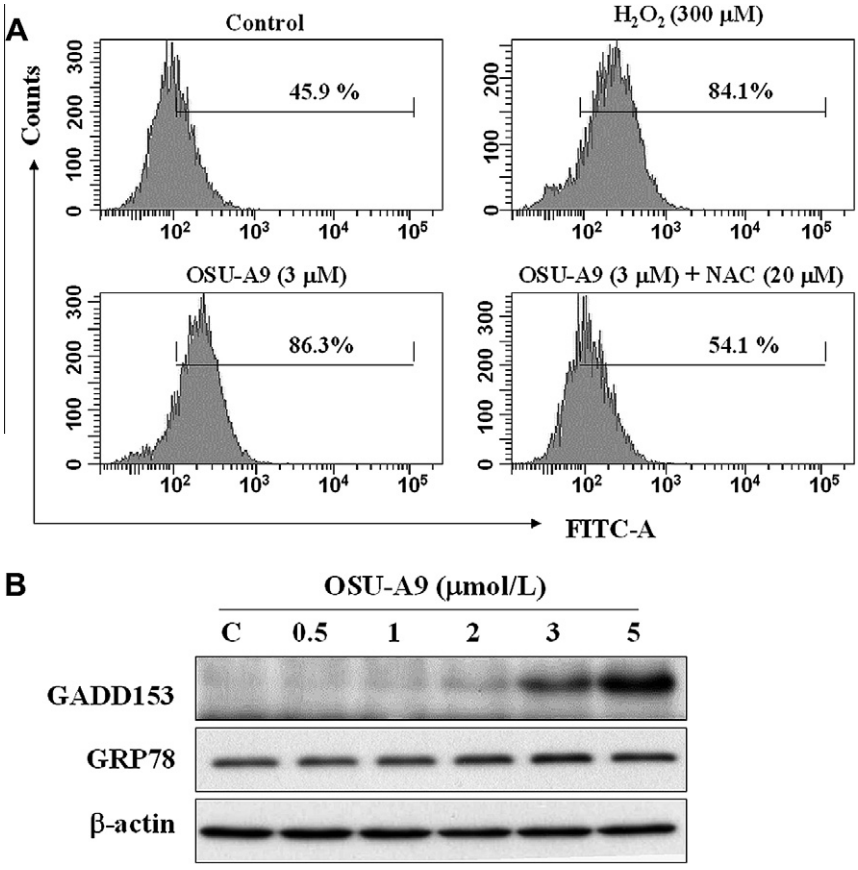

Figure 5 Reactive oxygen species and endoplasmic reticulum (ER) stress analysis in SCC2095 cells. Cells treated with DMSO or OSU-A9 for 48 h were stained with DCFH-DA (A). Western blotting of proteins involved in ER stress (B).

NF-κB is considered to be an important target for anticancer therapy since, compared with normal epithelial cells, oral cancer cells usually express higher constitutive levels which contribute to a malignant phenotype.[18–20] NF-κB also regulates the expression of many genes that are important for cell protection from radiation and chemotherapy, anti-apoptosis, cell survival, tumorigenesis, and cancer metastasis.[21–24] By down regulating the NF-κB pathway, bortezomib and Trichostatin A have been shown to effectively inhibit the cell growth of head and neck squamous cell carcinoma.[19,25] It is known that IκB kinase (IKKα/β), as a heterodimer, is responsible for phosphorylation of IκBα. Phosphorylated IκBα is ubiquitinated and degraded followed by the translocation of NF-κB to the nucleus. The association of IKK proteins with tumorigenesis of oral cancer is reported. Tamatani and colleagues showed that human head and neck carcinoma cells have increased expression of IKKα protein that contributes to the enhanced NF-κB activity.[22] IKKα is also important in the differentiation and disease progression of squamous cell carcinoma.[26] A study by Takada et al. demonstrated the activity of I3C in myeloid and leukemia cells through inhibition of NF-κB and NF-κB-regulated gene expressions. Specifically, it was found that I3C inhibits IKK activation without alteration of IKKα and IKKβ protein expression.[13] In our experiments, OSU-A9 showed a potent decrease in both constitutive and inducible NF-κB activity. In addition, OSU-A9 resulted in down regulation of phosphorylated IκBα and subsequent NF-κB expression. More interestingly, the inhibition of IKKα and IKKβ protein expression by OSU-A9 was not observed with I3C treatment. Thus, it is possible that the mechanisms underlying the inhibition of the NF-κB pathway by OSU-A9 are different from those by I3C.

Increased ROS is implicated in inflammation, cardiovascular disease, stroke, aging process, and cell apoptosis.[27,28] Recent cumulative evidences suggest increased ROS as a strategy in anticancer therapy.[16,29] Our study showed that OSU-A9 increases the production of ROS that can be rescued by co-treatment with *N*-acetylcysteine, which is not reported previously in studies of I3C and OSU-A9. In theory, since mitochondria are important sources of ROS, the loss of mitochondria membrane potential ($\Delta\Psi m$) caused by OSU-A9 leads to ROS release, further contributing to cell apoptosis in concert with modulation of the Akt and NF-κB pathways.

In summary, OSU-A9 induces apoptotic cell death, down regulates Akt and NF-κB signaling, and increases generation of ROS and ER stress in oral cancer cells. Compared to its parent compound, I3C, OSU-A9 shows 100-fold higher anticancer potency with preservation of the pleiotropic activities which strongly suggests its value in oral squamous cell carcinoma therapy.

Conflict of interest statement

The authors declare no competing financial interests.

Acknowledgements

This work was supported in part by grants from the Taiwan Department of Health, China Medical University Hospital Cancer Research of Excellence (DOH99-TD-C-111-005), the National Science Council grant (NSC 96-2320-B-021-MY3), and the China Medical University (CMU95-270 and CMU96-046).

References

1. Vermorken JB, Remenar E, van Herpen C, Gorlia T, Mesia R, Degardin M, et al. Cisplatin, fluorouracil, and docetaxel in unresectable head and neck cancer. *N Engl J Med* 2007;**357**:1695–704.
2. Auborn KJ. Can indole-3-carbinol-induced changes in cervical intraepithelial neoplasia be extrapolated to other food components? *J Nutr* 2006;**136**:2676S–8S.
3. Hsu JC, Dev A, Wing A, Brew CT, Bjeldanes LF, Firestone GL. Indole-3-carbinol mediated cell cycle arrest of LNCaP human prostate cancer cells requires the induced production of activated p53 tumor suppressor protein. *Biochem Pharmacol* 2006;**72**:1714–23.
4. Saegusa M, Hashimura M, Kuwata T, Hamano M, Okayasu I. Induction of p16INK4A mediated by beta-catenin in a TCF4-independent manner: implications for alterations in p16INK4A and pRb expression during trans-differentiation of endometrial carcinoma cells. *Int J Cancer* 2006;**119**:2294–303.
5. Weng JR, Tsai CH, Kulp SK, Chen CS. Indole-3-carbinol as a chemopreventive and anti-cancer agent. *Cancer Lett* 2008;**262**:153–63.
6. Dahler AL, Rickwood D, Guminski A, Teakle N, Saunders NA. Indole-3-carbinol – induced growth inhibition can be converted to a cytotoxic response in the presence of TPA+Ca(2+) in squamous cell carcinoma cell lines. *FEBS Lett* 2007;**581**:3839–47.
7. Grose KR, Bjeldanes LF. Oligomerization of indole-3-carbinol in aqueous acid. *Chem Res Toxicol* 1992;**5**:188–93.
8. Reed GA, Peterson KS, Smith HJ, Gray JC, Sullivan DK, Mayo MS, et al. A phase I study of indole-3-carbinol in women: tolerability and effects. *Cancer Epidemiol Biomarkers Prev* 2005;**14**:1953–60.
9. Safe S, Papineni S, Chintharlapalli S. Cancer chemotherapy with indole-3-carbinol, bis(3′-indolyl)methane and synthetic analogs. *Cancer Lett* 2008;**269**:326–38.
10. Weng JR, Tsai CH, Kulp SK, Wang D, Lin CH, Yang HC, et al. A potent indole-3-carbinol derived antitumor agent with pleiotropic effects on multiple signaling pathways in prostate cancer cells. *Cancer Res* 2007;**67**:7815–24.
11. Omar HA, Sargeant AM, Weng JR, Wang D, Kulp SK, Patel T, et al. Targeting of the Akt-nuclear factor-kappa B signaling network by [1-(4-chloro-3-nitrobenzenesulfonyl)-1H-indol-3-yl]-methanol (OSU-A9), a novel indole-3-carbinol derivative, in a mouse model of hepatocellular carcinoma. *Mol Pharmacol* 2009;**76**:957–68.
12. Weng JR, Tsai CH, Omar HA, Sargeant AM, Wang D, Kulp SK, et al. OSU-A9, a potent indole-3-carbinol derivative, suppresses breast tumor growth by targeting the Akt-NF-kappaB pathway and stress response signaling. *Carcinogenesis* 2009;**30**:1702–9.
13. Takada Y, Andreeff M, Aggarwal BB. Indole-3-carbinol suppresses NF-kappaB and IkappaBalpha kinase activation, causing inhibition of expression of NF-kappaB-regulated antiapoptotic and metastatic gene products and enhancement of apoptosis in myeloid and leukemia cells. *Blood* 2005;**106**:641–9.
14. Chao WR, Yean D, Amin K, Green C, Jong L. Computer-aided rational drug design: a novel agent (SR13668) designed to mimic the unique anticancer mechanisms of dietary indole-3-carbinol to block Akt signaling. *J Med Chem* 2007;**50**:3412–5.
15. Kim I, Xu W, Reed JC. Cell death and endoplasmic reticulum stress: disease relevance and therapeutic opportunities. *Nat Rev Drug Discov* 2008;**7**:1013–30.
16. Fang J, Seki T, Maeda H. Therapeutic strategies by modulating oxygen stress in cancer and inflammation. *Adv Drug Deliv Rev* 2009;**61**:290–302.
17. Ron D. Translational control in the endoplasmic reticulum stress response. *J Clin Invest* 2002;**110**:1383–8.
18. Nakayama H, Ikebe T, Beppu M, Shirasuna K. High expression levels of nuclear factor kappaB, IkappaB kinase alpha and Akt kinase in squamous cell carcinoma of the oral cavity. *Cancer* 2001;**92**:3037–44.
19. Lun M, Zhang PL, Pellitteri PK, Law A, Kennedy TL, Brown RE. Nuclear factor-kappaB pathway as a therapeutic target in head and neck squamous cell carcinoma: pharmaceutical and molecular validation in human cell lines using Velcade and siRNA/NF-kappaB. *Ann Clin Lab Sci* 2005;**35**:251–8.
20. Didelot C, Barberi-Heyob M, Bianchi A, Becuwe P, Mirjolet JF, Dauca M, et al. Constitutive NF-kappaB activity influences basal apoptosis and radiosensitivity of head-and-neck carcinoma cell lines. *Int J Radiat Oncol Biol Phys* 2001;**51**:1354–60.
21. Schwartz SA, Hernandez A, Mark Evers B. The role of NF-kappaB/IkappaB proteins in cancer: implications for novel treatment strategies. *Surg Oncol* 1999;**8**:143–53.
22. Tamatani T, Azuma M, Aota K, Yamashita T, Bando T, Sato M. Enhanced IkappaB kinase activity is responsible for the augmented activity of NF-kappaB in human head and neck carcinoma cells. *Cancer Lett* 2001;**171**:165–72.
23. Kumar A, Takada Y, Boriek AM, Aggarwal BB. Nuclear factor-kappaB: its role in health and disease. *J Mol Med* 2004;**82**:434–48.
24. Rahman KM, Ali S, Aboukameel A, Sarkar SH, Wang Z, Philip PA, et al. Inactivation of NF-kappaB by 3,3′-diindolylmethane contributes to increased apoptosis induced by chemotherapeutic agent in breast cancer cells. *Mol Cancer Ther* 2007;**6**:2757–65.
25. Yao J, Duan L, Fan M, Wu X. NF-kappaB signaling pathway is involved in growth inhibition, G2/M arrest and apoptosis induced by Trichostatin A in human tongue carcinoma cells. *Pharmacol Res* 2006;**54**:406–13.
26. Nakayama H, Ikebe T, Shirasuna K. Effects of IkappaB kinase alpha on the differentiation of squamous carcinoma cells. *Oral Oncol* 2005;**41**:729–37.
27. Galleron S, Borderie D, Ponteziere C, Lemarechal H, Jambou M, Roch-Arveiller M, et al. Reactive oxygen species induce apoptosis of synoviocytes in vitro. Alpha-tocopherol provides no protection. *Cell Biol Int* 1999;**23**:637–42.
28. Lindsay DG. Diet and ageing: the possible relation to reactive oxygen species. *J Nutr Health Aging* 1999;**3**:84–91.
29. Cabello CM, Bair 3rd WB, Wondrak GT. Experimental therapeutics: targeting the redox Achilles heel of cancer. *Curr Opin Invest Drugs* 2007;**8**:1022–37.